

## **S.T. Yau High School Science Award**

### **Research Report**

#### **The Team**

Name of team member: Jialin Dong  
School: TTV Community Day School:  
City, Country: Irvine, California, USA

#### **Title of Research Report**

Study of Cycloidal Curves and The Application in Hydraulic Motor Design

#### **Date**

Aug 23, 2025

# Study of Cycloidal Curves and The Application in Hydraulic Motor Design

Jialin Dong

## Abstract

The research described in this paper is a part of the design and development of a compact and high-torque hydraulic motor for robotic arms. Traditional motors are too bulky to be installed on robotic arms. This paper presents new designs of hydraulic motors based on cycloidal curves. It presents the mathematically detailed generation of both epicycloidal and hypocycloidal curves, including the standard, shortened, and modified cycloids, for cycloidal gears and corresponding pin gears. The innovative design of hydraulic epicycloidal and hypocycloidal motors was described, including designs of gears and the oil distribution system. The comparison with traditional cycloidal motors is discussed, and the advantages of the new design, including compact size and high precision, are highlighted. A hydraulic motor for a subsea robotic arm was designed as a real industrial design case. Compact size, high output torque, and smooth spinning at low speeds were needed. The method presented was used to make a hypocycloidal motor with seven teeth on the inner gear. The designed motor was installed on a subsea robotic arm and has been operating in a subsea environment for over a year. This design case completely proves that the theory and design method proposed here are effective.

**Keywords:** Engineering Mechanics, Mechanical Engineering, Robotic Arm, Cycloidal Gear, Hydraulic Motor, Robotics.

## **Acknowledgement**

The research has been solely conducted by Jialin Dong, and the Research Report has been completed by Jialin Dong. The research topic, data acquisition, data analysis and computation, experimental design and implementation, and the writing of the thesis have all been conducted by Jialin Dong himself. The author would like to thank Prof. Jianfei Mu and Prof. Nigata Zhu for the discussion on the mathematical derivation of cycloidal curves. The author would also like to thank Mr. Richard Ho for the support in the manufacture of the motor prototype. The machining process has been outsourced to Cathaybot Tech., and all fees produced from the machining process are paid by Jialin Dong. Jialin Dong has applied for a patent in the United States for the product of this research, a Floating Male-Rotor Hypocycloidal Motor. The application certificate is attached in the supplemental materials.

United States patent application number: US19/188,060

The product of the research, a Floating Male-Rotor Hypocycloidal Motor, has been licensed to Cathaybot Tech. for applications on robotic arms. CathayBot pays Jialin Dong \$28 for each application of the product of this research. The signed contract is attached in the supplemental materials.

## **Commitments on Academic Honesty and Integrity**

We hereby declare that we

1. are fully committed to the principle of honesty, integrity and fair play throughout the competition.
2. actually perform the research work ourselves and thus truly understand the content of the work.
3. observe the common standard of academic integrity adopted by most journals and degree theses.
4. have declared all the assistance and contribution we have received from any personnel, agency, institution, etc. for the research work.
5. undertake to avoid getting in touch with assessment panel members in a way that may lead to direct or indirect conflict of interest.
6. undertake to avoid any interaction with assessment panel members that would undermine the neutrality of the panel member and fairness of the assessment process.
7. observe the safety regulations of the laboratory(ies) where we conduct the experiment(s), if applicable.
8. observe all rules and regulations of the competition.
9. agree that the decision of YHSA is final in all matters related to the competition.

**We understand and agree that failure to honour the above commitments may lead to disqualification from the competition and/or removal of reward, if applicable; that any unethical deeds, if found, will be disclosed to the school principal of team member(s) and relevant parties if deemed necessary; and that the decision of YHSA is final and no appeal will be accepted.**

*(Signatures of full team below)*

X Jialin Dong

Name of team member:

X

Name of team member:

X

Name of team member:

X Jianfei Mu

Name of supervising teacher:

## Table of Contents

	Contents
1. Introduction .....	1
2. Method-Mathematical Modeling of Cycloids.....	2
3. Hydraulic Cycloidal Motor Design .....	7
4. Results-Design Case.....	11
5. Discussion .....	13
6. Conclusion .....	14
References.....	16

# 1. Introduction

The cycloids, the curves traced by a point on a rolling circle, have captivated mathematicians since the Renaissance. Although their properties were hinted at in antiquity, serious study began in the 17th century. Galileo Galilei (1599) is often credited with naming the cycloids and attempting to calculate the area under one arch, though his results were approximate.(Stillwell, 1989) The curve's true mathematical exploration flourished during the "century of genius": Blaise Pascal (1658) solved key problems related to its area and centroid, while Christiaan Huygens (1659) discovered its property, using it to design pendulum clocks with improved accuracy. The cycloids became a battleground for calculus pioneers—Johann Bernoulli, Jakob Bernoulli, Gottfried Leibniz, and Isaac Newton—who tackled the Brachistochrone problem (1697), proving the cycloids' optimality as the "curve of fastest descent." The cycloids' applications in physics, engineering, and mathematics cemented their legacy as a cornerstone of classical mechanics and calculus. The rich history reflects both the beauty of pure mathematics and its profound utility.(Whitman 1943)

In cycloids' application, the cycloidal pinion gear transmission system (Cycloidal Drive Systems) (Litvin & Fuentes, 2004) utilizes the geometric properties of epicycloid and hypocycloid, achieving high-precision power transmission through precise meshing mechanisms. In the field of hydraulic motors and reducers, the cycloidal pinion gear transmission system is widely used due to its high efficiency and flexibility. For example, in single-stage reducers (Qi et al., 2024) (Naveen et al., 2020), their output efficiency can reach over 98%, significantly reducing energy consumption and enhancing production efficiency. This paper explores the theory of cycloids and cycloidal transmission, which would be used in the innovation of hydraulic motor design.

The core of cycloidal pinion transmission is the great role of mathematical modeling of cycloidal tooth shape in gear meshing (mesh). Characteristics of cycloidal transmission are as follows. (Huang et al., 2021) (Zhang et al., 2020)

## 1) Compact and Lightweight Design

The rotor (pin gear) and stator (cycloidal gear) utilize cycloidal profiles. The rotor performs planetary motion via an eccentric shaft, eliminating the need for multi-stage transmissions, drastically reducing size. Its compact layout allows lighter weight compared to gear or piston motors of equivalent power, making them ideal for space-constrained systems (e.g., AGVs, robotic joints (Mesmer et al., 2022)).

## 2) Structural symmetry

In order to meet the bidirectional rotation requirements of hydraulic motors, the cycloidal gear and pin gear are adopted with a symmetrical structure. Reversing fluid flow direction enables easy forward/reverse switching without additional mechanisms. Through the precise cooperation between the eccentric cycloidal gear and the pin gear, the stable output of the drive is ensured. Speed is adjustable from near-zero to hundreds of rpm and adaptable to diverse operational needs.

### 3) Low speed and high torque characteristics

The geometric properties of cycloidal gears enable significant torque generation even at low speeds (high torque-to-volume ratio), ideal for applications requiring heavy-load, low-speed operation (e.g., cranes, excavator slewing mechanisms). Continuous meshing of cycloidal teeth minimizes output pulsations, ensuring stable operation even at extremely low speeds (e.g., 1-2 rpm) without "crawling" effects.

### 4) High Mechanical Efficiency and Durability

Multiple contact points (typically 6-8) during meshing ensure even pressure distribution, reducing localized wear. Rolling friction dominance further enhances energy efficiency. Critical components (e.g., rotor, stator) use hardened steel or composites for wear resistance. Hydraulic oil provides direct lubrication, minimizing the frequency of maintenance needed.

Although the geometric problem of cycloidal gear is based on the parametric equation of a circle (positive and negative cosine trigonometric functions), its correct mathematical derivation becomes a great difficulty and challenge due to its dynamic coordinate transformation. In the second part of this paper, the mathematical derivation of cycloids is provided with details in standard, shortened, and modified versions, which leads to a whole theory to generate cycloid curves for gear design. The third part describes the way to design a cycloidal motor, followed by a design case study of a hypocycloidal motor. Then, the test results of the designed motor are presented and discussed.

## 2. Method-Mathematical Modeling of Cycloids

### (1) Basic Cycloids

Firstly, the mathematical cycloidal model needs to be established. The Epicycloidal and Hypocycloidal curves are mathematically described in the following two parts.

#### 1) Epicycloids

As shown in Figure 1, let the big circle (shown in the quarter) be the base one with radius  $R$ , and the small circle is the rolling one with radius  $r$ . The parametric equations (i.e., the coordinates of a point) for the base circle can be written as:

$$\begin{cases} x=R\cdot\cos\theta \\ y=R\cdot\sin\theta \end{cases} \quad (1)$$

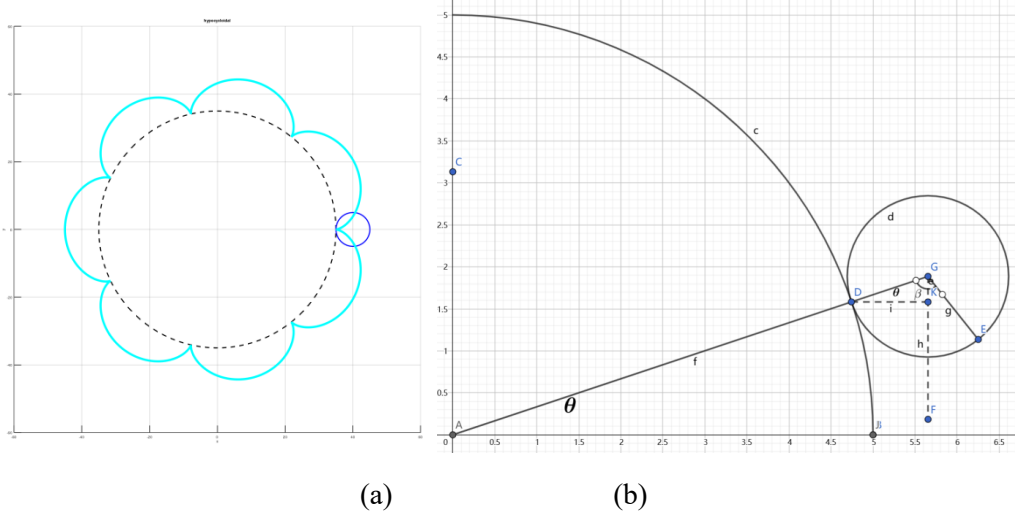


**Figure 1:** The geometric drawing of an epicycloidal curve. (a) The definition of a standard epicycloidal curve. (b) An enlarged drawing to describe the mathematical derivation.

Where  $\theta$  is the angle between the line connecting the point to the origin and the positive x-axis, the coordinates of the rolling circle's center are:

$$\begin{cases} x_r = (R+r) \cdot \cos \theta \\ y_r = (R+r) \cdot \sin \theta \end{cases} \quad (2)$$

When the rolling circle rolls on the base circle by an angle  $\theta$ , it rotates around its center by an angle. Because the rolling has no slipping, the arc lengths traced on the two circles are equal, i.e.,

$$R = z \cdot r \quad (3)$$

Here,  $z$  is an integer, which determines the number of petals of the cycloid, which is the number of teeth in a pin gear. Therefore, the coordinates of the reference point on the rolling circle are:

$$\begin{cases} x_e = x_r + r \cdot \sin \alpha \\ y_e = y_r - r \cdot \cos \alpha \end{cases} \quad (4)$$

Where,

$$\alpha = \angle EGF = \angle AGE - \angle AGF = \beta - \left(\frac{\pi}{2} - \theta\right) \quad (5)$$

Replacing  $x_r$ ,  $y_r$  and  $r$  by Eqns (2) and (3),

$$\begin{cases} x_e = r(z+1) \cdot \cos \theta + r \cdot \sin \left(\beta - \left(\frac{\pi}{2} - \theta\right)\right) \\ y_e = r(z+1) \cdot \sin \theta - r \cdot \cos \left(\beta - \left(\frac{\pi}{2} - \theta\right)\right) \end{cases} \quad (6)$$

Also, the arc  $\widehat{BD}$  is the same with arc  $\widehat{DE}$ , so

$$\theta \cdot R = \beta \cdot r \quad (7)$$

Finally, the expression of a standard epicycloid can be derived

$$\begin{cases} x_e = r(z+1) \cdot \cos\theta - r \cdot \cos[(1+z)\theta] \\ y_e = r(z+1) \cdot \sin\theta - r \cdot \sin[(1+z)\theta] \end{cases} \quad (8)$$

## 2) Hypocycloids

As shown in Figure 2 below, let the dashed line represent the base circle with radius, and the blue circle represent the rolling circle with radius  $r$ . The parametric equations (i.e., coordinates of a point) for the base circle can be expressed as Eqn (1):

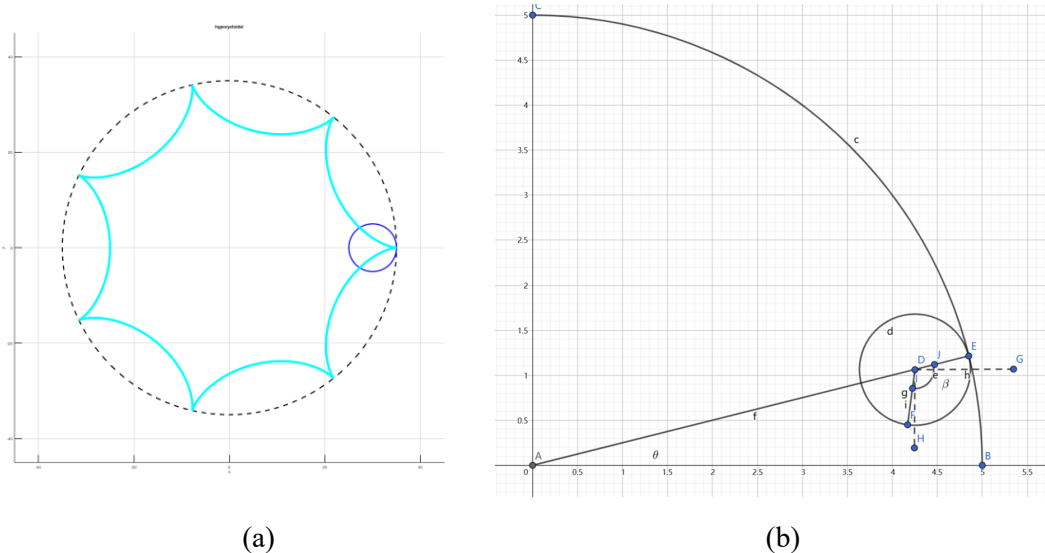


**Figure 2:** The geometric drawing of a hypocycloidal curve. (a) The definition of a standard hypocycloidal curve. (b) An enlarged drawing to describe the mathematical derivation.

The coordinates of the rolling circle's center are:

$$\begin{cases} x_r = (R-r) \cdot \cos\theta \\ y_r = (R-r) \cdot \sin\theta \end{cases} \quad (9)$$

When the rolling circle has rolled along the base circle by an angle  $\theta$ , it rotates around its center by an angle. Since the rolling has no slipping, the arc lengths traced on both circles are equal, i.e.,  $R$  and  $r$  have the same relation shown in Eqn(3),

Here,  $z$  is an integer that determines the number of lobes (petals) of the hypocycloid, corresponding to the number of teeth in the pin gear.

Thus, the coordinates of a reference point on the rolling circle are:

$$\begin{cases} x_h = x_r - r \cdot \sin\gamma \\ y_h = y_r - r \cdot \cos\gamma \end{cases} \quad (10)$$

Where,

$$\gamma = \angle HDF = \angle FDE - \angle HDE = \beta - \left(\frac{\pi}{2} + \theta\right) \quad (11)$$

Since the rolling circle moves on the base circle without sliding, the lengths of the arc  $\widehat{FE}$  and arc  $\widehat{BE}$  are the same, Eqn (12) is derived

$$R \cdot \theta = r \cdot \beta \quad (12)$$

After substituting Eqns (9, 11, 12) into Eqn (10), Eqn (13) can be obtained.

$$\begin{cases} x_h = r(z-1) \cdot \cos\theta - r \cdot \sin[\beta - (\frac{\pi}{2} + \theta)] \\ y_h = r(z-1) \cdot \sin\theta - r \cdot \cos[\beta - (\frac{\pi}{2} + \theta)] \end{cases} \quad (13)$$

This simplifies a standard hypocycloid to be expressed as:

$$\begin{cases} x_h = r(z-1) \cdot \cos\theta + r \cdot \cos[(z-1) \cdot \theta] \\ y_h = r(z-1) \cdot \sin\theta - r \cdot \sin[(z-1) \cdot \theta] \end{cases} \quad (14)$$

## (2) Revision and Modification

The standard cycloid has a serious flaw--it contains mathematically discontinuous points (non-differentiable points). To create a pin gear suitable for transmission, it's necessary to apply a displacement (offset) to create space for the rollers on the pin teeth to operate.

The method of displacement involves extending or shrinking the curve along its normal direction by a specific distance. Specifically, by calculating the differentials  $\{\frac{dx}{d\theta}, \frac{dy}{d\theta}\}$  at a given point, the proportional components in the x and y directions can be determined. The displacement is then applied according to the ratio of these components over the total displacement distance, as follows:

$$\begin{cases} l_x = l \cdot \frac{\frac{dx}{d\theta}}{\sqrt{\frac{dx^2}{d\theta} + \frac{dy^2}{d\theta}}} \\ l_y = l \cdot \frac{\frac{dy}{d\theta}}{\sqrt{\frac{dx^2}{d\theta} + \frac{dy^2}{d\theta}}} \end{cases} \quad (15)$$

However, because the standard cycloid has non-differentiable (discontinuous) points, it is impossible to calculate the displacement at these locations (see Figure 3).

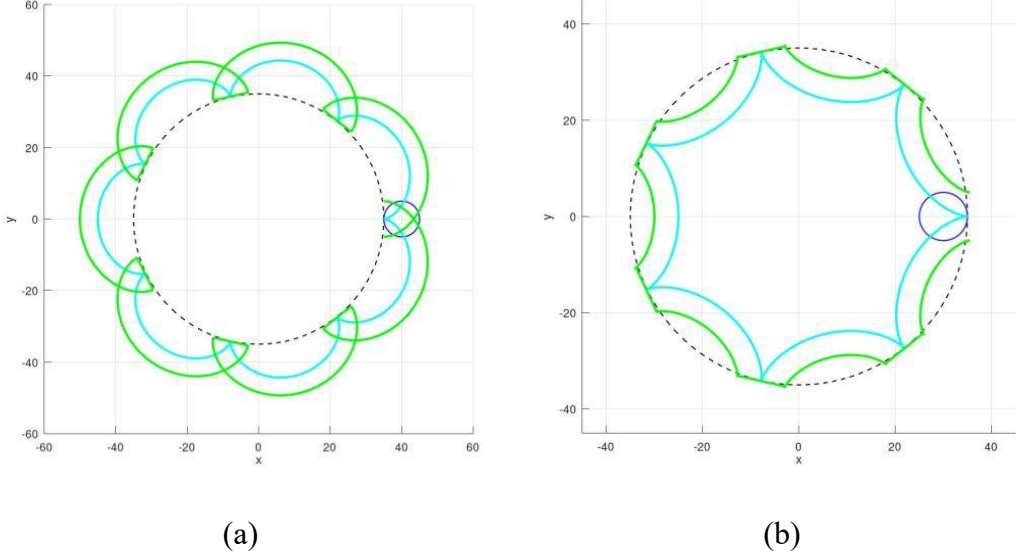


**Figure 3:** Modification of standard cycloidal curves: (a) Standard epicycloidal curves, and (b) Standard hypocycloidal curves

Thus, the standard cycloidal curves need to be revised. By replacing the in the subtracted term with  $\eta \cdot r$ , where  $\eta$  is a percentage less than 100% (i.e., using a point inside the rolling circle instead of on its circumference), a shortened epicycloid can be generated. In conclusion, the equations of the shortened epicycloids and hypocycloids can be derived as Eqn (16) and (17)

$$\begin{cases} x_{es} = r(z+1) \cdot \cos\theta - \eta \cdot r \cdot \cos[(1+z)\theta] \\ y_{es} = r(z+1) \cdot \sin\theta - \eta \cdot r \cdot \sin[(1+z)\theta] \end{cases} \quad (16)$$

$$\begin{cases} x_{hs} = r(z-1) \cdot \cos\theta + \eta \cdot r \cdot \cos[(z-1)\theta] \\ y_{hs} = r(z-1) \cdot \sin\theta - \eta \cdot r \cdot \sin[(z-1)\theta] \end{cases} \quad (17)$$

Next, the shortened cycloid in red in the graph is scaled equidistantly to form the green modified cycloids. This process uses proportional scaling: for a segment on the cycloid, its x- and y-direction components are scaled according to their proportional ratios given by Eqns (18) and (19).

$$\begin{cases} x_{em} = x_{es} - l \cdot \frac{\frac{dx_{es}}{d\theta}}{\sqrt{\frac{dx_{es}^2}{d\theta} + \frac{dy_{es}^2}{d\theta}}} = r(z+1) \cdot \cos\theta - \eta \cdot r \cdot \cos[(1+z)\theta] - l \cdot \frac{\frac{dx_{es}}{d\theta}}{\sqrt{\frac{dx_{es}^2}{d\theta} + \frac{dy_{es}^2}{d\theta}}} \\ y_{em} = y_{es} - l \cdot \frac{\frac{dy_{es}}{d\theta}}{\sqrt{\frac{dx_{es}^2}{d\theta} + \frac{dy_{es}^2}{d\theta}}} = r(z+1) \cdot \sin\theta - \eta \cdot r \cdot \sin[(1+z)\theta] - l \cdot \frac{\frac{dy_{es}}{d\theta}}{\sqrt{\frac{dx_{es}^2}{d\theta} + \frac{dy_{es}^2}{d\theta}}} \end{cases} \quad (18)$$

$$\begin{cases} x_{hm} = x_{hs} + l \cdot \frac{\frac{dx_{hs}}{d\theta}}{\sqrt{\frac{dx_{hs}^2}{d\theta} + \frac{dy_{hs}^2}{d\theta}}} = r(z-1) \cdot \cos\theta + \eta \cdot r \cdot \cos[(z-1) \cdot \theta] + l \cdot \frac{\frac{dx_{hs}}{d\theta}}{\sqrt{\frac{dx_{hs}^2}{d\theta} + \frac{dy_{hs}^2}{d\theta}}} \\ y_{hm} = y_{hs} + l \cdot \frac{\frac{dy_{hs}}{d\theta}}{\sqrt{\frac{dx_{hs}^2}{d\theta} + \frac{dy_{hs}^2}{d\theta}}} = r(z-1) \cdot \sin\theta - \eta \cdot r \cdot \sin[(z-1) \cdot \theta] + l \cdot \frac{\frac{dy_{hs}}{d\theta}}{\sqrt{\frac{dx_{hs}^2}{d\theta} + \frac{dy_{hs}^2}{d\theta}}} \end{cases} \quad (19)$$

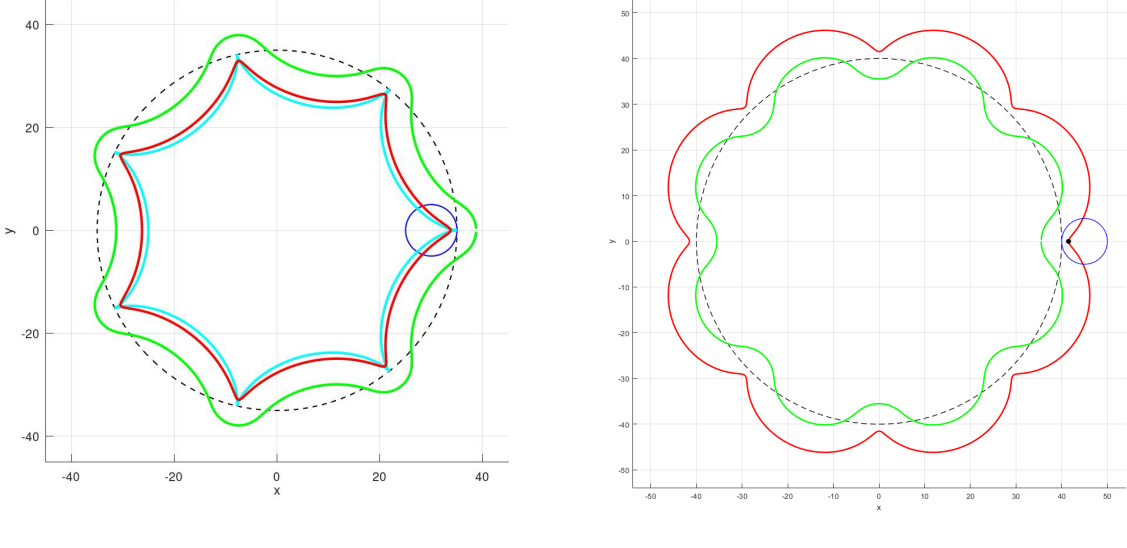


**Figure 4:** Modification of shortened cycloidal curves: (a) Shortened epicycloidal curves, and (b) Shortened hypocycloidal curves

### 3. Hydraulic Cycloidal Motor Design

The author used the mathematical program in Octave to generate the cycloidal gear and pin gear's shape, and CAD software to make a 3D model of the motor. Before giving the details on how to design two types of motors in the following two parts, three concepts need to be defined: rotor, stator, and float stator.

**Rotor** is the inner gear, which can spin along the central axis.

**A Stator** is a part that cannot spin and is normally fixed to the housing.

**The float stator** is the outer gear that is not spinning but movable to adjust the contact position with the rotor so that mechanical transmission can be achieved.

#### (1) Epicycloidal Gear and Pin Gear Design

The epicycloidal gear is an inner gear, i.e., rotor. The design is based on Eqn (18). The equation can be used to generate an epicycloidal curve with four parameters: radius of rolling circle  $r$ , integer ratio of base circle to rolling circle  $z$  (i.e., the number of petals), shorten coefficient  $\eta$ , and displacement distance  $l$ . The curve, which is shown as the green curve in Figure 5(a), forms

the contact surface of a cycloidal gear. For an epicycloidal hydraulic motor, the cycloidal gear is the inner gear, while the pin gear is the outer gear, which can be seen in Figure 5(b).

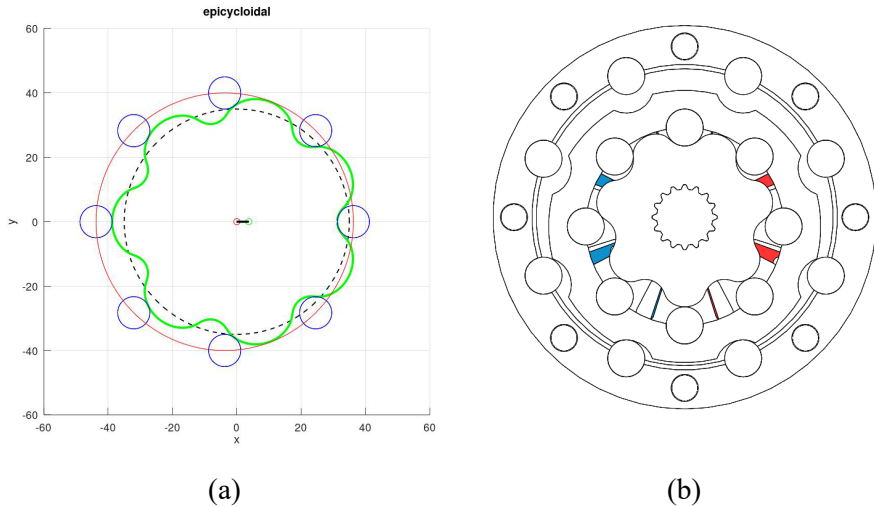


**Figure 5:** Epicycloidal motor design. (a) Gear curves generation. (b) Use the generated curve to design a motor in 3D CAD software

The pin gear is the outer gear, i.e., the float stator, and is formed by several pins, which are tangent to the epicycloidal curve. Also, it is eccentric to the curve, and the eccentric offset is the shortened radius to form the curve  $0102=\eta \cdot r$ . Therefore, there are  $z+1$  circular teeth shown as the blue circles in Figure 5(a) located on a circle eccentric to the origin, which is shown as the red circle. These cylinders are just tangent to the epicycloid. There are two methods to design the pin gear after determining the epicycloidal curve: mathematical and engineering methods.

**Mathematical Method.** The small red and green circles are the center of the red circle and the green curve, respectively. The red circle is

$$\begin{cases} x_{epb} = (R+r) \cdot \cos \theta - \eta \cdot r \\ y_{epb} = (R+r) \cdot \sin \theta \end{cases} \quad (20)$$

The  $i$ -th pin on the pin gear can be expressed as

$$\begin{cases} x_{epc\_i} = l \cdot \cos(\theta) + (R+r) \cdot \cos(2\pi/(z+1) \cdot (i-1)) - \eta \cdot r \\ y_{epc\_i} = l \cdot \sin(\theta) + (R+r) \cdot \sin(2\pi/(z+1) \cdot (i-1)) \end{cases} \quad (21)$$

**Engineering Method.** In CAD software, place cylinders equispaced with a radius of  $l$  tangent to the epicycloid from outside, which is shown in Figure 5(b).

## (2) Hypocycloidal Gear and Pin Gear Design

Similar to epicycloidal gear, the hypocycloidal gear design is based on Eqn (19). However, it is the outer gear, i.e., the float stator. The equation can be used to generate a hypocycloid with four parameters: radius of rolling circle  $r$ , integer ratio of base circle to rolling circle  $z$  (i.e., the

number of petals), shortening coefficient  $\eta$ , and displacement distance  $l$ . The curve, which is shown as the green curve in Figure 6(a), forms the contact surface of a cycloidal gear.

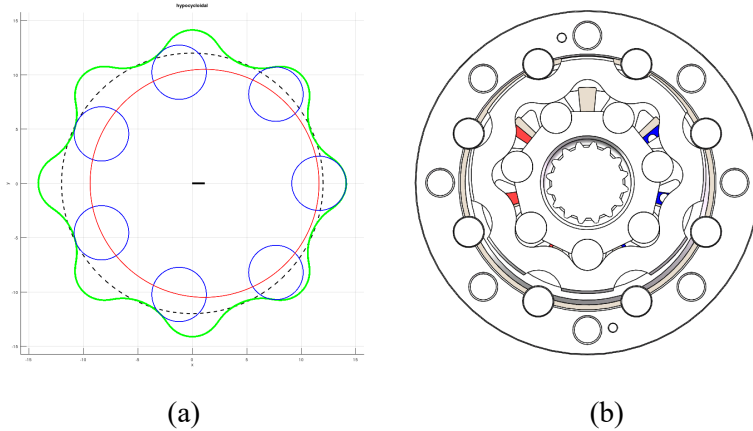


**Figure 6:** Hypocycloidal motor design. (a) Gear curves generation. (b) Use the generated curve to design a motor in 3D CAD software.

The pin gear is formed by several pins, which are tangent to the hypocycloid from inside. It is eccentric to the curve, and the eccentric offset is the shortened radius to form the curve  $0102=\eta \cdot r$ . Differently, the pin gear in a hypocycloidal motor is a rotor. There are  $z+1$  circular teeth shown as the blue circles in Figure 6(a) located on a circle eccentric to the origin, which is shown as the red circle. These cylinders are just tangent to the epicycloid. There are two methods to design a pin gear after determining the hypocycloid: mathematical and engineering methods.

**Mathematical Method.** The small red and green circles are the center of the red circle and the green curve, respectively. The red circle is

$$\begin{cases} x_{hp} = (R-r) \cdot \cos \theta + \eta \cdot r \\ y_{hp} = (R-r) \cdot \sin \theta \end{cases} \quad (22)$$

and the  $i$ -th pin on the pin gear can be expressed as

$$\begin{cases} x_{hpc\_i} = l \cdot \cos(\theta) + (R-r) \cdot \cos(2\pi/z \cdot (i-1)) + \eta \cdot r \\ y_{hpc\_i} = l \cdot \sin(\theta) + (R-r) \cdot \sin(2\pi/z \cdot (i-1)) \end{cases} \quad (23)$$

**Engineering Method.** Similarly, in CAD software, place cylinders equispaced with a radius tangent to the hypocycloid from the inner side, as shown in Figure 6(b).

### (3) Oil Distribution Design

It can be seen from Figure 5 and Figure 6 that a pair of rotor and float stator of both epicycloidal and hypocycloidal motors creates cavities, each of which is formed by two pins, a segment of curve on the cycloid, and a segment of curve on the pin gear. The only difference is

that the cycloidal curve segment of the hypocycloidal motor is outside, while that of the epicycloidal motor is inside.

When the rotors of both motors spin, half (if the number of cavities is even) or nearly half (if the number of cavities is odd) cavities tend to be enlarged, and the others are the contrary. For example, when the rotor of the epicycloidal motor shown in Figure 5 spins clockwise, the cavities with blue marks get smaller. The volume of a cavity turns to decreases when it crosses the upper half of the vertical bisector. On the other hand, the cavity's volume increases when it crosses the lower half of the vertical bisector. Therefore, the oil distribution is easily implemented by the following theory.

**Oil Distribution Theory:** After deciding the direction to spin, the oil distribution system always fills the cavities, which tend to be larger with high-pressure oil, and allows the ones that tend to be smaller to output oil back to the low-pressure tank.

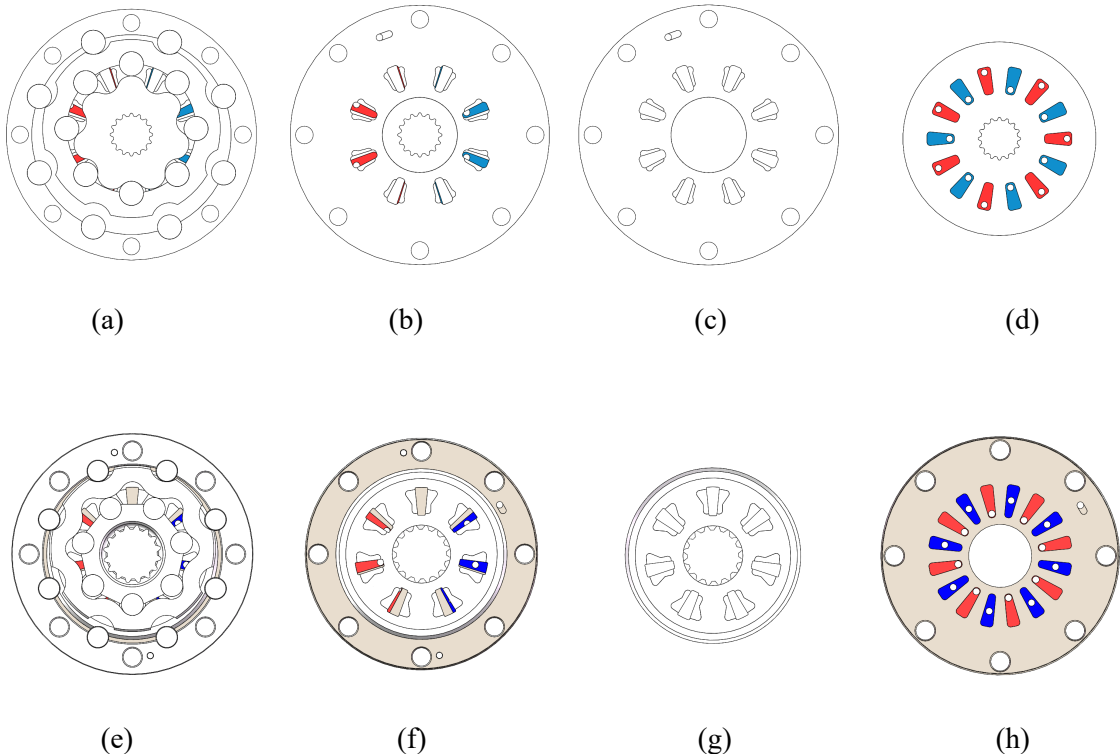


**Figure 7:** The oil distribution systems of epicycloidal and hypocycloidal motors. The first row is 3D models of an epicycloidal motor, while the second row is those of a hypocycloidal motor. (a) and (e) are epicycloidal and hypocycloidal motors. (b) and (f) are the oil distribution systems of both motors. (c) and (g) are the oiling plates. (d) and (h) are the distributing plates

The oil distribution system consists of two parts: the oiling plate and the distributing plate. The oiling plate is the one that contacts both gears and fills oil into the cavities. The distributing plate is the one that contacts and rotates relatively to the oiling plate. Since there is a relative rotation between these two plates, the cavities would either be filled with oil or output oil according to the relative angle.

Figure 7 shows the oil distribution systems of two types of motors. It can be found that the number of oiling holes is equal to the number of teeth of the pin gears. The number of distributing holes is twice the number of cycloidal gears. Table 1 shows a summary of the design issues of both motors.

**Table 1:** Summary of the structure of epicycloidal and hypocycloidal motors. It provides a description of the basic structure used in design and the key parameters determined as design input.

Item	Epicycloidal Motor	Hypocycloidal Motor
Inner Gear	Cycloidal Gear	Pin Gear
Outer Gear	Pin Gear	Cycloidal Gear
Oiling Plate	Stationery to Housing	Stationary to Rotor
Distributing Plate	Stationary to Rotor	Stationery to Housing
Number of Teeth, Inner Gear	$z$	$z$
Number of Teeth, Outer Gear	$z+1$	$z+1$
No. of Oiling Holes	$z+1$	$z$
No. of Distributing Holes	$2z$	$2(z+1)$

Comparing the oil distribution systems of both motors, the epicycloidal motor is more difficult to design. An oiling hole shall always be between two pins. However, the pin gear of the epicycloidal motor is a floating part, which slides in the housing. Therefore, oiling holes should be sized and located to guarantee that it is always between two pins, even when the pin gear is sliding, which is a difficulty that does not exist in a hypocycloidal motor.

## 4. Results-Design Case

After analyzing the mathematical model of two cycloidal curves and discussing the design of oil distribution systems, a motor can be easily designed and manufactured. Firstly, for a subsea manipulator, a hypocycloidal motor was determined to be designed and used. The limited size of such manipulators requires the diameter of our motor to be less than 110mm. After a brief sketch, a diameter of around 50mm for our base circle is determined. The design starts with the sketch and then iterates according to the design result. The specifications are listed in Table 2.

Assume the base circle radius is  $R=25\text{mm}$ . The number of inner gear teeth is  $z=7$ , and, therefore, the one of outer gear teeth is  $z+1=8$ . The radius of the rolling circle is  $r=\frac{R}{z}=3.57\text{mm}$ . The author selects the eccentric distance  $r_s=2.5\text{mm}$ , and thus the shortening coefficient is  $\eta=\frac{r_s}{r}=0.7$ . To use standard bearing rollers,  $l=5\text{mm}$  is determined. Figure 8 shows the design and machined parts.

**Table 2:** Specification parameters of the designed hypocycloidal motor, including the symbol definitions and the values used in the design.

Parameter	Symbol	Value
Radius of base circle	$R$	25mm
Radius of rolling circle	$r$	3.57mm
Shorten coefficient	$\eta$	0.7
Displace	$l$	5mm
Radius of roller	$r_r$	5mm
No. of teeth, pin gear	$z$	7
No. of teeth, cycloidal gear	$z+1$	8
Eccentric distance	$O1O2$	2.5mm
Thickness of gear	$b$	20mm
Volume displacement	$V_Q$	116ml/rev

The motor is assembled and tested on a dynamometer. The motor is installed on the dynamometer, and the spline shaft is connected to a magnetic adjustable load. The motor is powered by a pressure-controlled hydraulic power unit and controlled by a servo valve. The input pressure, spinning speed, and flow are all monitored. The test results are achieved and shown in Table 3. According to the design specification, the theoretical output torque is

$$\tau = \frac{P * V_Q}{2\pi} = 387.7 \text{Nm}$$

The test results show that the efficiency of the motor is

$$\eta_e = \frac{330}{387.7} = 85\%$$

The performance of the low-speed high-torque (LSHT) motor is good. The special structure makes each cavity change the status of filling and discharging by  $z \cdot (z+1)$  times, which is equivalent to a  $z \cdot (z+1):1$  reducer. It can run smoothly when the speed is 3 rpm, which is very useful for extremely low-speed applications such as robotic joints.



**Figure 8:** The design process. (a) the design in CAD software, (b) the machined and assembled gears, and (c) the subsea manipulator, the wrist of which is equipped with the hypocycloidal motor.

**Table 3:** Test results of the designed hypocycloidal motor, which represent the performance of the motor. These are important parameters to evaluate a motor.

Displacement	Maximum Speed	Continuous Flow Rate/ Instantaneous Flow Rate	Continuous Pressure Instantaneous Pressure	Continuous Torque Instantaneous Torque	Maximum Power
116ml/rev	716 rpm	70L/min 80L/min	14MPa 21MPa	278Nm 330Nm	26.5HP

## 5. Discussion

Traditional cycloidal motors normally use an inner epicycloidal gear, a pin gear, and a spline coupler. The innovative application of a floating stator replacing a spline coupler makes the presented motors superior to traditional cycloidal motors. The main advantages are as follows:

- (1) The motor length in the axial direction is dramatically decreased. In a traditional motor, the outer gear and housing are the same part, which is fixed. As presented in the mathematical part, the inner gear needs to spin eccentrically if the outer gear is fixed. The traditional one needs to use a coupler with splines at each end, shown in Figure 9, which requires extra length (even more than double the length) in the axial direction.
- (2) Since one end of the coupler needs to spin with sliding movement in a traditional motor, the spline cannot be too tight, which means that the backlash is big, and the accuracy is not high enough for precise servo control.

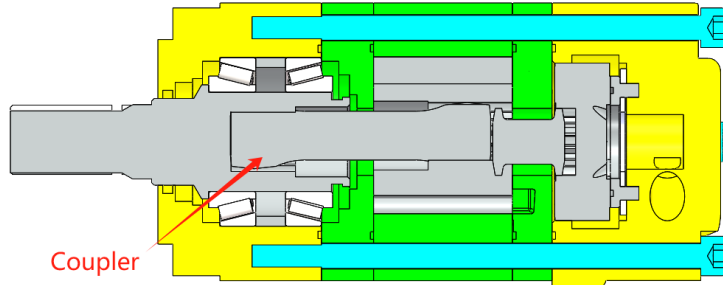


**Figure 9:** A traditional epicycloidal motor. It is clear that such kind of motor has large size in axial dimension due to using coupler to transmit motion

On the other hand, the only drawback of the presented epicycloidal motor is slightly larger in the radial direction compared to the traditional cycloidal motor. However, the presented hypocycloidal motor can also help reduce that size. The hypocycloidal motor designed and presented in this paper has been used in the subsea manipulator shown in Figure 8(c) due to its compact size and large torque output. The subsea manipulator has been working at a depth of 4500 meters shown in Figure 10.



**Figure 10** Operation at 4500msw

## 6. Conclusion

This paper presents mathematically detailed generation of both epicycloidal and hypocycloidal curves, including the standard, shortened, and modified cycloids, for designing cycloidal gears and corresponding pin gears. It provides not only the mathematical formulas but also the process to design gears. Moreover, the innovative design of hydraulic epicycloidal and hypocycloidal motors is described. Especially, the oil distribution system is analyzed and compared to traditional cycloidal motors. The critical contribution in this paper is motor design with a hypocycloid, which is rarely published. The advantages of the presented design are obvious. It can achieve a more compact size and more precise transmission.

A real industrial design case was also presented in this paper. A hydraulic motor was required by a subsea robotic arm. Compact size, high output torque, and smooth spinning at low speeds were needed. The method presented in this paper was used to make a hypocycloidal motor

with seven teeth on the inner gear, 2.5mm eccentric distance, and a 20mm gear thickness. The maximum output torque is reached at a pressure of 21 MPa. When the machining precision was guaranteed, it could smoothly spin at the speed of 1.5rpm. The designed motor was installed on a subsea robotic arm and has been working in a subsea environment for more than a year. This design case completely proves that the theory and design method proposed here are effective.

## References

Huang, J., Li, C., Zhang, Y., Wang, Y., & Chen, B. (2021). Transmission error analysis of cycloidal pinwheel meshing pair based on rolling – sliding contact. *Journal of the Brazilian Society of Mechanical Sciences and Engineering*, 43(7). <https://doi.org/10.1007/s40430-021-03074-6>

Litvin, F. L., & Fuentes, A. (2004). *Gear Geometry and Applied Theory*. <https://doi.org/10.1017/cbo9780511547126>

Mesmer, P., Nagel, P., Lechler, A., & Verl, A. (2022). Modeling and Identification of Hysteresis in Robot Joints with Cycloidal Drives. *2022 IEEE 17th International Conference on Advanced Motion Control (AMC)*, 358 – 363. <https://doi.org/10.1109/amc51637.2022.9729274>

Naveen, P., Kiran, R., Siva Sankaram, E. V. S., & Bharadwaj, T. M. (2020). Design, Analysis and Simulation of Compact Cycloidal Drive. *International Journal of Scientific Research in Science, Engineering and Technology*, 216 – 220. Internet Archive. <https://doi.org/10.32628/ijsrset207547>

Qi, L., Yang, D., Cao, B., Li, Z., & Liu, H. (2024). Design principle and numerical analysis for cycloidal drive considering clearance, deformation, and friction. *Alexandria Engineering Journal*, 91, 403 – 418. <https://doi.org/10.1016/j.aej.2024.01.077>

Stillwell, J. (1989). Complex Numbers and Functions. In: *Mathematics and Its History*. Undergraduate Texts in Mathematics. Springer, New York, NY. [https://doi.org/10.1007/978-1-4899-0007-4\\_15](https://doi.org/10.1007/978-1-4899-0007-4_15)

Whitman, E. A. (1943). Some historical notes on the cycloid. *The American Mathematical Monthly*, 50(5), 309-315. <https://doi.org/10.1080/00029890.1943.11991383>

Zhang, T., Li, X., Wang, Y., & Sun, L. (2020). A Semi-Analytical Load Distribution Model for Cycloid Drives with Tooth Profile and Longitudinal Modifications. *Applied Sciences*, 10(14), 4859. <https://doi.org/10.3390/app10144859>